

Fast bit flipping based on stability transition of coupled spins

Maximilian F. I. Kieler[✉] and Arnd Bäcker[✉]

Technische Universität Dresden, Institut für Theoretische Physik and Center for Dynamics, 01062 Dresden, Germany

 (Received 16 January 2023; accepted 19 July 2023; published 8 August 2023)

A bipartite spin system is proposed for which a fast transfer from one defined state into another exists. For sufficient coupling between the spins, this implements a bit-flipping mechanism, which is much faster than that induced by tunneling. The states correspond in the semiclassical limit to equilibrium points with a stability transition from elliptic-elliptic stability to complex instability for increased coupling. The fast transfer is due to the spiraling characteristics of the complex unstable dynamics. Based on the classical system we find an approximate scaling relation for the transfer time, which even applies in the deep quantum regime. By investigating a simple model system, we show that the classical stability transition is reflected in a fundamental change in the structure of the eigenfunctions.

DOI: [10.1103/PhysRevE.108.L022203](https://doi.org/10.1103/PhysRevE.108.L022203)

Introduction. The concept of quantum computing [1] enables new possibilities of future computational devices. Despite a lot of recent progress, quantum computing will not supersede classical computing, instead they are expected to complement each other [2,3]. Thus, it is important to investigate current quantum computation realizations for the ability of implementing classical operations. A fundamental requirement of information processing is a fast and energy efficient switching between two (quantum) states $|0\rangle$ and $|1\rangle$. From a many-body perspective, this could be realized, for example, by using spintronics [4–6]. Another approach is to employ few-body systems, which should be realizable with current experimental devices, e.g., using ultracold atoms [7–9]. Such many-body systems differ from spin $\frac{1}{2}$ systems by having a semiclassical limit and, thus, can be investigated by more intuitive classical methods. For example, a transfer between two specific states can be realized using dynamical tunneling [10–13] between symmetry related regions. However, the tunneling time for such a quantum process approximately depends inversely on the energy difference of the two states, hence demanding for a compromise between energy efficiency and switching speed. Thus, it is an interesting open question to devise systems for which both goals can be reached simultaneously.

In this paper, we present a mechanism for bit flipping in a system of two coupled spins, which is both fast and energy efficient. We implement the states representing the bits by antiparallel aligned coherent states [14,15] of the spin system, i.e., $|0\rangle \equiv |\rightleftharpoons\rangle$, $|1\rangle \equiv |\leftrightsquigarrow\rangle$. In the classical limit of large spins, the quantum system becomes a dynamical system, and the states can be classically described by initial conditions, which are localized around the equilibrium points of the system. Depending on the parameters the stability of these equilibrium points changes from elliptic-elliptic (EE) stability to complex instability (CU) [16,17]. The characteristic feature of a complex unstable equilibrium is a spiraling dynamics in the neighborhood leading to a fast repulsion away from the equilibrium point [18–21]. As the dynamics is

confined to the surface of Bloch spheres for each subsystem, the spiraling motion transfers the state from one side to the antipodal side. This classical transfer is also reflected in the quantum time evolution of the state $|\rightleftharpoons\rangle$, which transforms into the bit-flipped state $|\leftrightsquigarrow\rangle$. The transfer to $|\leftrightsquigarrow\rangle$ can be quantified using the fidelity [22], see Fig. 1. We establish, based on classical arguments, a universal behavior in system size using a rescaled time. Using a simplified system, which embodies the essential aspects of the stability transition, we demonstrate that this is connected with a fundamental change in the structure of the eigenfunctions from localized to nonlocal.

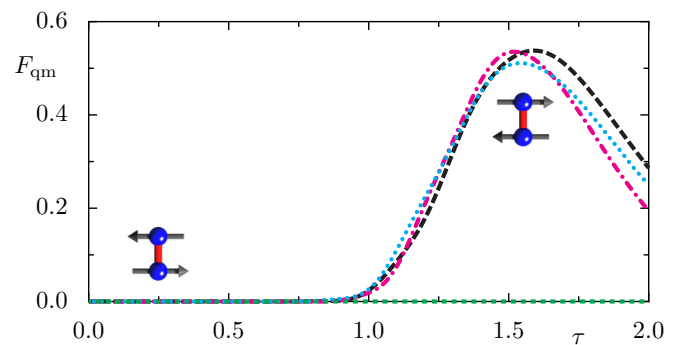


FIG. 1. Quantum transfer from $|0\rangle \equiv |\rightleftharpoons\rangle$ to $|1\rangle \equiv |\leftrightsquigarrow\rangle$ as measured by the fidelity (2) for different parameters (j, k, ϵ) as $(25, 1.0, 1.2)$ for the black dashed line, $(40, 1.0, 1.2)$ for the magenta dash-dotted line, and $(25, 1.2, 1.4)$ for the cyan dotted line. The transfer for different parameters follows the same curve by using the rescaled time τ , see Eq. (9), which is the actual time divided by the time of the analytical approximation, explained in more detail in the main text below. The green dashed curve with $F_{\text{qm}} \approx 0$ is for $(j, k, \epsilon) = (15, 1.0, 0.8)$ where only dynamical tunneling occurs. The fast bit flipping for the first sets of parameters semiclassically corresponds to complex unstable dynamics (defined below), whereas, no transfer occurs for elliptic-elliptic stability.

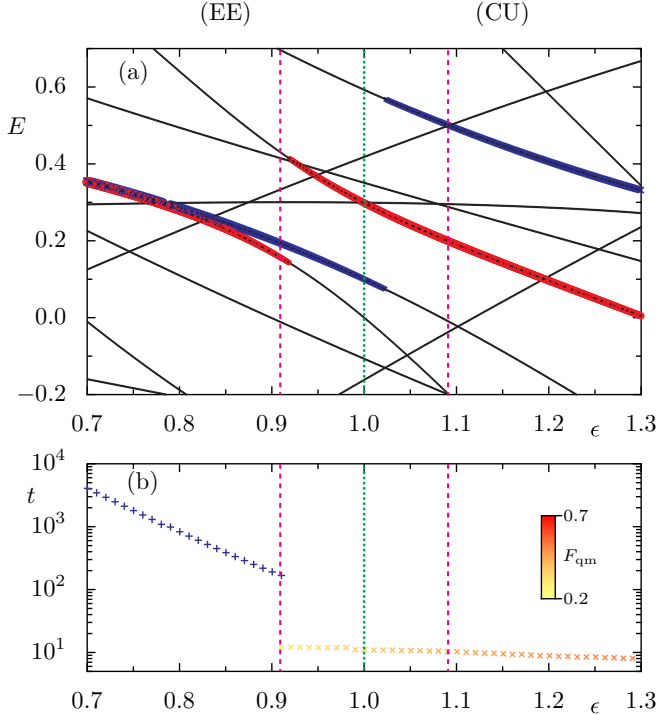


FIG. 2. (a) Relevant energy levels as function of the coupling ϵ : Red lines highlight those levels, whose eigenfunctions have maximal overlap with $|\rightleftharpoons\rangle$, and blue lines highlight those with $|\leftrightsquigarrow\rangle$. (b) Dynamical tunneling time t_{dyn} (blue +) for $\epsilon < \epsilon_{\text{crit}} = 1$ and the transfer time t_{trans} (yellow to orange x) for $\epsilon > \epsilon_{\text{crit}}$, see Eq. (4) on the semilogarithmic scale. The fidelity at time t_{trans} is encoded by color. The green vertical dotted line indicates the critical coupling strength $\epsilon_{\text{crit}} = 1.0$, and the red vertical dashed lines indicate the parameter regime $\epsilon_{\text{crit}} \mp 1/N$ for $N = 11$ ($j = 5$).

Quantum system. We consider a bipartite system of two coupled spins,

$$H = J_x^{(1)} + \frac{k_1}{2j_1} (J_z^{(1)})^2 + J_x^{(2)} + \frac{k_2}{2j_2} (J_z^{(2)})^2 + \frac{\epsilon}{\sqrt{j_1 j_2}} J_z^{(1)} J_z^{(2)}, \quad (1)$$

where $J^{(i)} = (J_x^{(i)}, J_y^{(i)}, J_z^{(i)})$ is the spin operator of the subsystems $i = 1, 2$. For simplicity, we restrict ourselves to spins of equal size, $j_1 = j_2 = j$, giving rise to subsystem Hilbert spaces of dimension $N = 2j + 1$. For numerical illustrations, $k_1 = k_2 = k = 1.0$ is used (unless explicitly mentioned). The parameter ϵ imposes a coupling of the two subsystems, each being a variant of the Lipkin-Meshkov-Glick model [23]. Note that system (1) is an autonomous version of the coupled kicked tops [24,25]. It can also be written in terms of Bose-Hubbard operators [26,27] and experimentally be realized in its time-periodically driven version [9].

The bit-states $|0\rangle$ and $|1\rangle$ are realized by two spin-coherent product states [14,15,26]. The first state $|0\rangle \equiv |\rightleftharpoons\rangle$ aligns both angular momenta antiparallel in the x direction, i.e., the first spin in the positive and the second in the negative x direction, see Fig. 3. The second state $|1\rangle \equiv |\leftrightsquigarrow\rangle$ is the spin-flipped counterpart. The time evolution is given by the unitary time evolution operator $U(t) = e^{-iHt}$, and we quantify the quan-

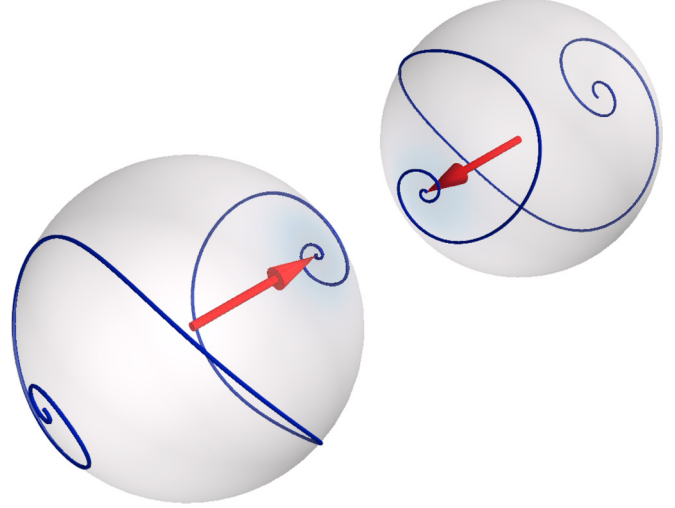


FIG. 3. Classical motion of the initial state $|\rightleftharpoons\rangle$ indicated by red arrows in the two Bloch spheres. A spiraling motion towards the antipodal point leads to the spin-flipped state $|\leftrightsquigarrow\rangle$.

tum transfer from $|0\rangle$ to $|1\rangle$ by the fidelity between the time evolved state $|\leftrightsquigarrow(t)\rangle = U(t)|\leftrightsquigarrow\rangle$ and the fixed bit-flipped state $|\leftrightsquigarrow\rangle$,

$$F_{\text{qm}}(t) = |\langle \leftrightsquigarrow | \leftrightsquigarrow(t) \rangle|^2. \quad (2)$$

Therefore, $F_{\text{qm}}(t = 0) = 0$ and a full transfer to the bit-flipped state would correspond to $F_{\text{qm}}(t_{\text{trans}}) = 1$. It turns out that there is a parameter range of the coupling ϵ for which there is essentially no transfer. However, increasing the coupling beyond some critical parameter ϵ_{crit} , see Eq. (4) below, a fast and significant transfer takes place, illustrated in Fig. 1. We point out that this is not a full transfer of the state, but it is sufficient to be reliably detectable. In the following, we explain the mechanism underlying this transfer.

The quantum dynamics of the bipartite quantum system (1) is determined by the eigenvalue equation $H|\Psi_n\rangle = E_n|\Psi_n\rangle$. Therefore, a representation of the energy levels E_n as function of the coupling ϵ for a small system $j = 5$, see Fig. 2, provides an intuitive understanding of the mechanism: For the time evolution, $U(t) = \sum_n e^{-iE_n t} |\Psi_n\rangle \langle \Psi_n|$, only those eigenstates are relevant, which are related to the states $|\rightleftharpoons\rangle$ and $|\leftrightsquigarrow\rangle$. Due to the antiparallel structure of the spins in $|\rightleftharpoons\rangle$ and $|\leftrightsquigarrow\rangle$, the sum of the energies of the identical subsystems is approximately zero so that we can concentrate on the middle of the spectrum only. The eigenstates, which are most relevant for the transfer from $|\rightleftharpoons\rangle$ to $|\leftrightsquigarrow\rangle$ can be identified by computing the overlap of $|\rightleftharpoons\rangle$ and $|\leftrightsquigarrow\rangle$ with all eigenstates, respectively, e.g., $|\langle \leftrightsquigarrow | \Psi_n \rangle|^2$. In Fig. 2(a), we present the energy levels, whose eigenfunctions have the maximal overlap with $|\rightleftharpoons\rangle$ in blue and with $|\leftrightsquigarrow\rangle$ in red. First, we focus on the parameter regime $\epsilon < k$ for which the overlap of $|\leftrightsquigarrow\rangle$ and $|\rightleftharpoons\rangle$ occurs mainly with two eigenstates only. In this parameter regime, the two states are in a semiclassical description (see below) located within symmetry-related regular regions in phase space so that dynamical tunneling [10–13] between them is possible. This situation can be described by an effective two-level system with eigenfunctions of the form of $|\Psi_{\pm}\rangle := \frac{1}{\sqrt{2}}(|\rightleftharpoons\rangle \pm |\leftrightsquigarrow\rangle)$. The tunneling time is determined

by $t_{\text{dyn}} = 2\pi/|E_+ - E_-|$. However, as the considered pair of energy levels is nearly degenerate, the tunneling time becomes very large, see Fig. 2(b), hence, a transfer from $|\leftrightarrow\rangle$ to $|\leftrightsquigarrow\rangle$ by dynamical tunneling would require extremely long times. This is seen in Fig. 1 where the fidelity remains essentially zero in the considered time interval.

By increasing the coupling to $\epsilon \sim k$, the system starts to behave differently. The state distributes over multiple eigenfunctions with larger energy gaps and the approximation by a two-level system becomes invalid. Hence, the dynamical tunneling time does not provide a suitable estimate in the transition regime. For the parameter regime $\epsilon \gtrsim k$, the transfer time $t_{\text{trans}} = \max(F_{\text{qm}})$, i.e., the time to reach the first maximum, is numerically computed using the fidelity Eq. (2). This transition occurs much faster than for dynamical tunneling, see Fig. 2(b). Note that the dynamical tunneling time is the time to reach the first global maximum and is, therefore, different from the transfer time, which is the time to reach the first maximum. In Fig. 2, the fidelity achieved at the transfer time is indicated by color. This shows that for having both short transfer time and large fidelity one needs $\epsilon > 1$. Moreover, as the initial and final states still only have a small energy difference, the transfer can be performed with less energy than, for example, in a single spin system where the energy difference between opposite spin configurations is much larger.

While dynamical tunneling for $\epsilon < k$ is a purely quantum effect, in contrast, the transfer for $\epsilon > k$ is of classical origin and can be approached by semiclassical methods.

Semiclassical description. By considering the semiclassical limit of the quantum spin to a classical angular momentum leads to a dynamical system. Using the mean-field approach, see, e.g., Ref. [26], of replacing operators by c numbers and taking the limit $j \rightarrow \infty$ we obtain from Eq. (1) the system of differential equations,

$$\begin{aligned} \dot{x}_1 &= -k_1 y_1 z_1 - \epsilon y_1 z_2, \\ \dot{y}_1 &= -z_1 + k_1 x_1 z_1 + \epsilon x_1 z_2, \\ \dot{z}_1 &= y_1, \\ \dot{x}_2 &= -k_2 y_2 z_2 - \epsilon y_2 z_1, \\ \dot{y}_2 &= -z_2 + k_2 x_2 z_2 + \epsilon x_2 z_1, \\ \dot{z}_2 &= y_2. \end{aligned} \quad (3)$$

The pairs of coordinates (x_i, y_i, z_i) for $i = 1, 2$, each lie on the surface of a unit Bloch sphere. Thus, the system (3) can be mapped by a canonical transformation $(\phi_i, z_i) = [\sqrt{1 - z_i^2} \arctan(y_i/x_i), z_i]$ into a system, which is effectively four dimensional with coordinates $(\phi_1, z_1, \phi_2, z_2)$. In this classical description, the coherent states $|\leftrightarrow\rangle$ and $|\leftrightsquigarrow\rangle$ turn into equilibrium points of (3), i.e., $|\leftrightarrow\rangle$ corresponds to $(x_1, y_1, z_1; x_2, y_2, z_2) = (1, 0, 0; -1, 0, 0)$ and $|\leftrightsquigarrow\rangle$ to $(-1, 0, 0; 1, 0, 0)$, respectively. Thus, the quantum transfer from $|\leftrightarrow\rangle$ to $|\leftrightsquigarrow\rangle$ can be investigated in terms of the classical dynamics of orbits in the neighborhood of these equilibrium points. The stability of such orbits is determined by the linearized dynamics, which is characterized by the four stability eigenvalues λ_ℓ of the stability matrix [16]. Depending on the system parameters a transition from elliptic-elliptic (EE)

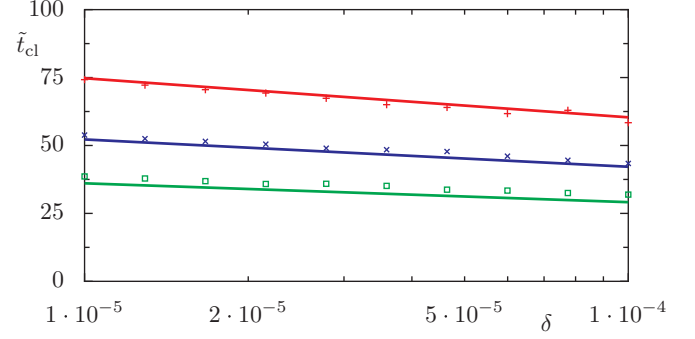


FIG. 4. Numerically computed average time of an ensemble of orbits, which are a spherical distance δ on the Bloch sphere away from the equilibrium point corresponding to $|\leftrightarrow\rangle$ to reach the equator of the sphere. The solid lines show $\epsilon = 1.05, 1.1, 1.2$ (red, blue, and green from top to bottom).

stability to complex unstable (CU) dynamics occurs for the critical parameter,

$$\epsilon_{\text{crit}} = \frac{k_1 + k_2}{2}. \quad (4)$$

The elliptic stability for $\epsilon < \epsilon_{\text{crit}}$ is characterized by purely imaginary eigenvalues. As the local dynamics effectively corresponds to $e^{\lambda t}$, the dynamics is rotational and stays in a bounded neighborhood of the equilibrium, hence, classically no spin flip is possible. In the CU parameter regime $\epsilon > \epsilon_{\text{crit}}$, the four eigenvalues λ_ℓ form a so-called Krein-quartet $(\pm\lambda, \pm\lambda^*)$ with some complex $\lambda = c_1 + ic_2$. This leads to a logarithmic spiraling motion [18–21], see Fig. 3 where the expanding motion is determined by the real part c_1 and the rotation by c_2 . As a consequence, orbits in the neighborhood of the equilibrium are no longer confined. In particular, an orbit reaching the equator of the Bloch sphere spirals inwards to the antipodal side, thus, provides a classical transfer, similar to the quantum transfer. To obtain an analytical estimate of the classical transfer time, we model the quantum dynamics by classical orbits starting a distance $\delta = \sqrt{\delta_1^2 + \delta_2^2}$ away from an equilibrium point and determine the time \tilde{t}_{cl} when they reach the equator at $x_1 = x_2 = 0$. By using the symmetry of the transfer the total time is $2\tilde{t}_{\text{cl}}$. One gets a logarithmic dependence of the classical transfer time,

$$\tilde{t}_{\text{cl}}(\delta) = \frac{1}{c_1 c_2} \ln \left(\frac{\pi}{2\delta} \right), \quad (5)$$

where

$$c_1, c_2 = \sqrt{\frac{\sqrt{\epsilon^2 + k_1 - k_2 - k_1 k_2 + 1}}{2} \mp \frac{(2 + k_1 - k_2)}{4}}. \quad (6)$$

Figure 4 demonstrates that this estimate gives good agreement with the numerical results obtained from the classical ensemble for various widths δ and different coupling ϵ . For the final step towards a semiclassical description, we consider the quantum coherent states as a Gaussian distribution for each subsystem, which is centered around the equilibrium point with variance $\sigma^2 = \frac{2}{N}$. Hence, we obtain after averaging the initial conditions by such a radial normal

distribution,

$$t_{\text{cl}} = \frac{1}{\sigma^4} \int_0^\infty dr_1 \int_0^\infty dr_2 2r_1 r_2 \tilde{t}_{\text{cl}}(x) e^{-(r_1^2 + r_2^2)/(2\sigma^2)} \quad (7)$$

$$= \frac{1}{c_1 c_2} \left[\ln \left(\frac{\pi^2}{8\sigma^2} \right) + \gamma - 1 \right], \quad (8)$$

where $\gamma = 0.5772 \dots$ is the Euler-Mascheroni constant.

Using the classical transfer time (8) allows for establishing an approximate scaling relation of the quantum transfer with respect to the system size $N = 2j + 1$ by using the rescaled time,

$$\tau = \frac{t}{t_{\text{cl}}}. \quad (9)$$

Thus, for a fixed coupling ϵ , the transfer scales similarly for different angular momenta j in the rescaled time as illustrated in Fig. 1 where also a parameter set is depicted with different values of k and ϵ . This rescaling works well only for not too large differences of $\epsilon - k$. Remarkably, the transfer scales logarithmic in N and is, thus, of the same order as the Ehrenfest time, which quantifies the time how long quantum dynamics is expected to follow classical motion. Consequently, the universal transfer even works in the deep quantum regime of small sized spins $j \approx 5$.

Note that the change in the quantum transfer time is not abrupt at $\epsilon = \epsilon_{\text{crit}}$ but extends over the parameter interval $\epsilon_{\text{crit}} \pm 1/N$, indicated by the vertical dashed red lines in Fig. 2.

Model system with complex instability. The mechanism of the transfer described for the system of two coupled angular momenta relies on the possibility for complex instability, but also on the phase space organization. Thus, in order to better understand the nature of the EE to CU transition itself, we focus on the Cherry Hamiltonian, which is locally similar to the coupled spin system. For this, we consider the semiclassical limit of the Hamiltonian (1) by using canonical coordinates. By a Taylor expansion of the Hamiltonian in one of the equilibrium points, we obtain a system which locally reproduces the elliptic-elliptic to complex unstable transition. Such a transition in its simplest form occurs for the Cherry Hamiltonian, which we use for further analysis. The classical Cherry Hamiltonian [28] describing two coupled harmonic oscillators,

$$H_{\text{cherry}} = \frac{1}{2}(p_1^2 + q_1^2) - \frac{w}{2}(p_2^2 + q_2^2) + \mu p_1 p_2, \quad (10)$$

where $w > 0$. The two coupled harmonic oscillators have opposite signs in their subsystems energy. As a consequence, the equilibrium at $(p_1, p_2, q_1, q_2) = (0, 0, 0, 0)$ exhibits a EE-CU transition for $\mu_{\text{crit}} = \frac{1-w^2}{2\sqrt{w}}$. The negative energy scale of one subsystem has important consequences on the energy level organization for which we consider the case of small detuning of the oscillators $\Delta := |w - 1| \ll 1$: For an uncoupled system of finite subsystem size M , we find energy levels the energy levels are $E_{n_1, n_2} = n_1 - w n_2 + 1/2 - w/2$ with $n_\ell = 0, \dots, M - 1$, see Fig. 5. Thus the levels are given by clusters $\alpha = n_1 - n_2$, which are itself similar to a single harmonic oscillator with frequency Δ . Provided that each cluster is well separated to the neighboring ones, only the level interactions within a cluster are important. Hence, we consider such a single harmonic cluster described by an effective Hamilto-

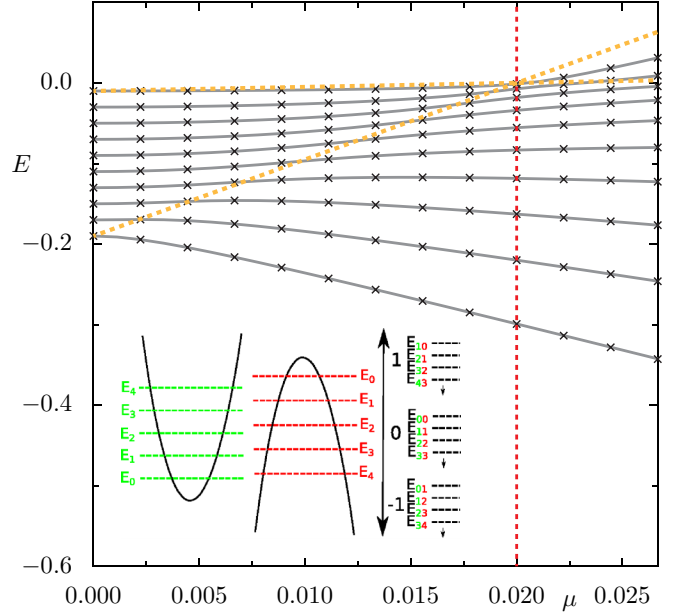


FIG. 5. Energy levels of the quantized Hamiltonian (10) for $M = 10$ (crosses), compared to the effective Hamiltonian (11) (lines) for a single cluster $\alpha = 0$ and $\Delta = 0.02$. The red dashed vertical line indicates the EE-CU transition, yellow dashed lines are the boundaries imposed by the Geršgorin circle theorem (only upper bounds). The inset illustrates how the energy clusters arise for the uncoupled case.

nian,

$$H_{\text{cluster}} = -\Delta \sum_{m=1}^M m |m\rangle \langle m| + \sum_{m=2}^M \frac{\mu m}{2} (|m\rangle \langle m-1| + |m-1\rangle \langle m|). \quad (11)$$

This reproduces the essential behavior of the Cherry Hamiltonian at the EE-CU transition, see Fig. 5. In the basis $\{|m\rangle\}$, the Hamiltonian is represented by a tridiagonal matrix. The Geršgorin circle theorem [29], simplified to this special case, Eq. (11), states that all eigenvalues have to lie within the union of intervals with lengths given by the sum of the off-diagonal matrix rows, centered around the value of the diagonal entry. This provides boundaries to the range of the eigenvalues. We observe that the upper constraint from the lowest and the highest energy cross at $\mu = \Delta$, see the yellow lines in Fig. 5, which is close to the transition point of the classical system, leading to a larger range of the eigenvalues in the CU regime. The crossing in which the highest and lowest eigenvalues are connected, already indicates a transition and, thus, establishes some kind of long-ranged correlation. This becomes more explicit by considering the “ground state” of the system, which is the eigenstate with largest eigenvalue. We find that this state is exponentially localized in the EE regime and becomes delocalized at the transition point (not shown). In the EE regime, the state can be described as an exponentially localized vector $|\Psi\rangle = \sum c_j |\Psi_j\rangle$ with $c_j \sim e^{-j/l}$ and localization length l . Using this ansatz in Eq. (11) leads to

a self-consistent expression for l , which diverges at the critical point,

$$l = \frac{1}{\ln\left(\frac{\Delta}{\mu} + \sqrt{\left(\frac{\Delta}{\mu}\right)^2 - 1}\right)}. \quad (12)$$

This diverging localization length results in a delocalized eigenfunction. This delocalization in the simplified system can be seen as the corresponding effect for the spin system (1) where the initial state becomes distributed over multiple eigenstates. The classical interpretation of this effect can be understood by the spiraling motion of orbits, which are no longer confined and explore a large region of phase space.

Summary and outlook. For two opposing equilibrium points of the proposed bipartite system (1) changing the coupling induces a transition from elliptic-elliptic stability to complex unstable dynamics in the semiclassical limit. The counter-rotating, bipartite nature of the initial state

configuration and the geometry of phase space allows for a fast and energy-efficient transfer from the state $|\overleftarrow{\rightleftharpoons}\rangle$ into the bit-flipped state $|\overrightarrow{\rightleftharpoons}\rangle$ compared to dynamical tunneling. These results can also be extended to the case of a time-periodic kicked system, namely, the coupled kicked tops for which we obtain qualitatively similar results. Of future interest is the situation of parameters, which are directly on the transition boundary, where a power-law dependence of the transition time is expected. We propose an experimental investigation of the system either as a kicked or as an autonomous realization. Particularly interesting would be to extend the system to multiple bits, which would allow for investigating the emergence of complex instability in many-body systems, such as in Bose-Hubbard systems, which have a semiclassical limit.

Acknowledgments. We thank T. Herrmann, R. Ketzmerick, and J. R. Schmidt for useful discussions. Funded by the Deutsche Forschungsgemeinschaft (DFG, German Research Foundation) Grants No. 290128388 and No. 497038782.

-
- [1] M. A. Nielsen and I. L. Chuang, *Quantum Computation and Quantum Information* (Cambridge University Press, Cambridge, UK, 2010).
- [2] A. Peruzzo, J. McClean, P. Shadbolt, M.-H. Yung, X.-Q. Zhou, P. J. Love, A. Aspuru-Guzik, and J. L. O'Brien, A variational eigenvalue solver on a photonic quantum processor, *Nat. Commun.* **5**, 4213 (2014).
- [3] J. R. McClean, J. Romero, R. Babbush, and A. Aspuru-Guzik, The theory of variational hybrid quantum-classical algorithms, *New J. Phys.* **18**, 023023 (2016).
- [4] S. Bhatti, R. Sbiaa, A. Hirohata, H. Ohno, S. Fukami, and S. N. Piramanayagam, Spintronics based random access memory: A review, *Mater. Today* **20**, 530 (2017).
- [5] V. Baltz, A. Manchon, M. Tsoi, T. Moriyama, T. Ono, and Y. Tserkovnyak, Antiferromagnetic spintronics, *Rev. Mod. Phys.* **90**, 015005 (2018).
- [6] I. Žutić, J. Fabian, and S. Das Sarma, Spintronics: Fundamentals and applications, *Rev. Mod. Phys.* **76**, 323 (2004).
- [7] I. Bloch, J. Dalibard, and S. Nascimbène, Quantum simulations with ultracold quantum gases, *Nat. Phys.* **8**, 267 (2012).
- [8] M. Albiez, R. Gati, J. Fölling, S. Hunsmann, M. Cristiani, and M. K. Oberthaler, Direct Observation of Tunneling and Non-linear Self-Trapping in a Single Bosonic Josephson Junction, *Phys. Rev. Lett.* **95**, 010402 (2005).
- [9] J. Tomkovič, W. Muessel, H. Strobel, S. Löck, P. Schlagheck, R. Ketzmerick, and M. K. Oberthaler, Experimental observation of the Poincaré-Birkhoff scenario in a driven many-body quantum system, *Phys. Rev. A* **95**, 011602(R) (2017).
- [10] M. J. Davis and E. J. Heller, Quantum dynamical tunneling in bound states, *J. Chem. Phys.* **75**, 246 (1981).
- [11] S. Keshavamurthy and P. Schlagheck, *Dynamical Tunneling: Theory and Experiment* (Taylor and Francis, Boca Raton, FL, (2011).
- [12] D. A. Steck, W. H. Oskay, and M. G. Raizen, Observation of chaos-assisted tunneling between islands of stability, *Science* **293**, 274 (2001).
- [13] E. J. Heller, *The Semiclassical Way to Dynamics and Spectroscopy* (Princeton University Press, Princeton, 2018).
- [14] A. Perelomov, *Generalized Coherent States and Their Applications*, Theoretical and Mathematical Physics (Springer-Verlag, Berlin/Heidelberg, 1986).
- [15] W.-M. Zhang, D. H. Feng, and R. Gilmore, Coherent states: Theory and some applications, *Rev. Mod. Phys.* **62**, 867 (1990).
- [16] J. E. Howard and R. S. Mackay, Calculation of linear stability boundaries for equilibria of hamiltonian systems, *Phys. Lett. A* **122**, 331 (1987).
- [17] C. Skokos, On the stability of periodic orbits of high dimensional autonomous Hamiltonian systems, *Physica D* **159**, 155 (2001).
- [18] D. C. Heggie, Bifurcation at complex instability, *Celestial Mech.* **35**, 357 (1985).
- [19] G. Contopoulos, S. C. Farantos, H. Papadaki, and C. Polymilis, Complex unstable periodic orbits and their manifestation in classical and quantum dynamics, *Phys. Rev. E* **50**, 4399 (1994).
- [20] J. Stöber and A. Bäcker, Geometry of complex instability and escape in four-dimensional symplectic maps, *Phys. Rev. E* **103**, 042208 (2021).
- [21] P. A. Patsis, T. Manos, L. Chaves-Velasquez, C. Skokos, and I. Puerari, Chaoticity in the vicinity of complex unstable periodic orbits in galactic type potentials, *Physica D* **429**, 133050 (2022).
- [22] R. Jozsa, Fidelity for mixed quantum states, *J. Mod. Opt.* **41**, 2315 (1994).
- [23] H. J. Lipkin, N. Meshkov, and A. J. Glick, Validity of many-body approximation methods for a solvable model: (I). Exact solutions and perturbation theory, *Nucl. Phys.* **62**, 188 (1965).
- [24] P. A. Miller and S. Sarkar, Signatures of chaos in the entanglement of two coupled quantum kicked tops, *Phys. Rev. E* **60**, 1542 (1999).
- [25] J. N. Bandyopadhyay and A. Lakshminarayan, Entanglement production in coupled chaotic systems: Case of the kicked tops, *Phys. Rev. E* **69**, 016201 (2004).

- [26] M. P. Strzys, E. M. Graefe, and H. J. Korsch, Kicked Bose–Hubbard systems and kicked tops—destruction and stimulation of tunneling, *New J. Phys.* **10**, 013024 (2008).
- [27] A. Micheli, D. Jaksch, J. I. Cirac, and P. Zoller, Many-particle entanglement in two-component Bose-Einstein condensates, *Phys. Rev. A* **67**, 013607 (2003).
- [28] T. M. Cherry, On periodic solutions of Hamiltonian systems of differential equations, *Phil. Trans. R. Soc. A* **227**, 137 (1928).
- [29] S. Geršgorin, Über die Abgrenzung der Eigenwerte einer Matrix, *Bulletin de l’Académie des Sciences de l’URSS, Classe des sciences mathématiques et na* **6**, 749 (1931).